Supporting Information

Thieno[3,2-*c*]pyran: ESIPT based fluorescence "turn–on" molecular chemosensor for selective recognition of Zn^{2+} ion and AIE property

Divya Singhal,[a] Ismail Althagafi,[b] Ashish Kumar,[a] Saroj Yadav,[a] Ashok K. Prasad[a] and Ramendra Pratap[a,*]

[a]Department of Chemistry, University of Delhi, North Campus, Delhi, India-110007
[b]Department of Chemistry, Umm Al-Qura University, Makkah, Saudi Arabia

E-mail ramendrapratap@gmail.com

X-ray Crystallography

The structure of chemosensor P was confirmed by single crystal diffraction analysis. The crystal suitable for X-ray diffraction studies were developed by slow evaporation of dichloromethane solution of P. The intensity data were collected at 298 K with an Oxford XCalibur CCD diffractometer equipped with a graphite monochromated Mo-Kα radiation (λ = 0.71073 Å). Data reduction was performed with the CrysAllisPro program (Oxford Diffraction ver. 171.34.40). The crystal structure was solved by direct methods using SHELXS-97 program and refined on F^2 using all data by full matrix least-squares procedures with SHELXL-97 within the OLEX-2 suite. The hydrogen atoms were placed at the calculated positions and included in the last cycles of the refinement. All calculations were done using the WinGX software package. Crystallographic data collection and structure solution parameters are summarized in Table 3. CCDC-2000213 contains the supplementary crystallographic data for this paper.

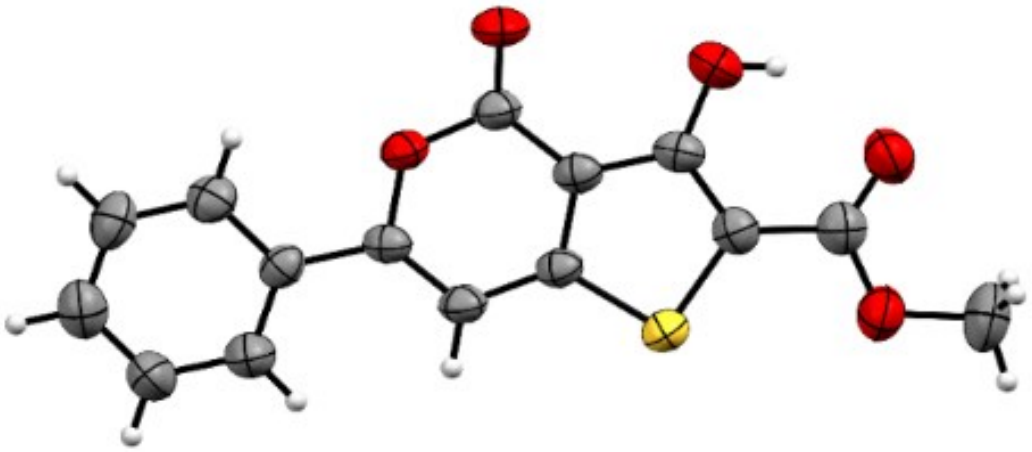

Fig. S1: Crystallography structure of chemosensor P.

Table S1: Crystal data and structure refinement for Probe P

CCDC Number	2000213
Identification code	2000213
Empirical formula	C15 H10 O5 S
Formula weight	302.29
Temperature	293(2) K
Wavelength	0.71073 Å
Crystal system	Orthorhombic
Space group	P c a 21
Unit cell dimensions	a = 13.2481(4) Å
α= 90°.	
	b = 8.2931(3) Å
	β= 90°.
	c = 12.1623(4) Å
	γ = 90°.
Volume	1336.25(8) $Å^3$
Z	4
Density (calculated)	1.503 Mg/m^3
Absorption coefficient	0.261 mm^{-1}
F(000)	624
Crystal size	0.22 x 0.20 x 0.18 mm^3
Theta range for data collection	3.502 to 29.518°.
Index ranges	18<=h<=18, -11<=k<=11, -16<=l<=16
Reflections collected	18574
Independent reflections	3407 [R(int) = 0.0434]
Completeness to theta = 25.242°	99.6 %
Refinement method	Full-matrix least-squares on F^2
Data / restraints / parameters	3407 / 1 / 190
Goodness-of-fit on F^2	0.648
Final R indices [I>2sigma(I)]	R1 = 0.0453, wR2 = 0.1124
R indices (all data)	R1 = 0.0728, wR2 = 0.1453
Absolute structure parameter	0.03(5)
Extinction coefficient	n/a
Largest diff. peak and hole	0.175 and -0.175 $e.Å^{-3}$

Hill Plot

The binding constant log β for P with Zn^{2+} ion was determined by Hill plot. A graph was plotted between log $[(I - I_0)/I_{max}\text{-}I]$ against log $[Zn^{2+}]$, where I, I_0 and I_{max} are the emission intensity of P, minimum and maximum intensity in the presence of metal ions respectively.

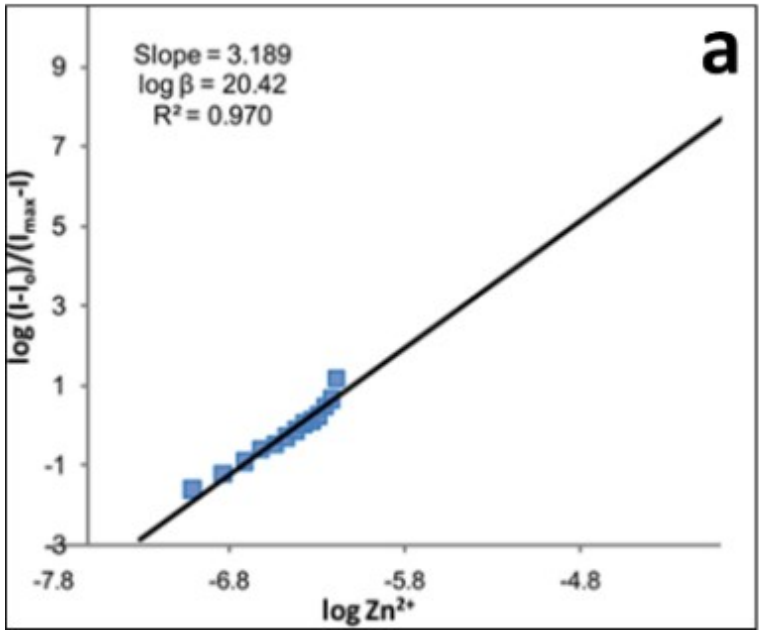

Fig. S2: Hill plot.

Concentration dependent emission spectra[1]

Moreover, the concentration-dependent fluorescence was studied for probe **P** to know the molecular form present in solution, which decide the fluorescence intensity variation. A concentration of 10^{-3} -10^{-9} M of probe P was maintained; at very low concentration, the band was occurred at 461 nm with extra band of 426 and 402 nm and on increasing the conc. a band of 484 nm was noted which became prominent (10^{-5} -10^{-9} M) whereas the maximum intensity was observed in 10^{-9} M solution **(Fig. S3)**. Hence, the fluorescence behaviour is sensitive to the concentration of the solution. On gradual increment of concentration, the intensity became somewhat significant, although these compounds were almost nonemissive in the solution state. Such occurrence can also be depicted by the fast intramolecular proton transfer process, which can serve as a nonradiative relaxation decay path.

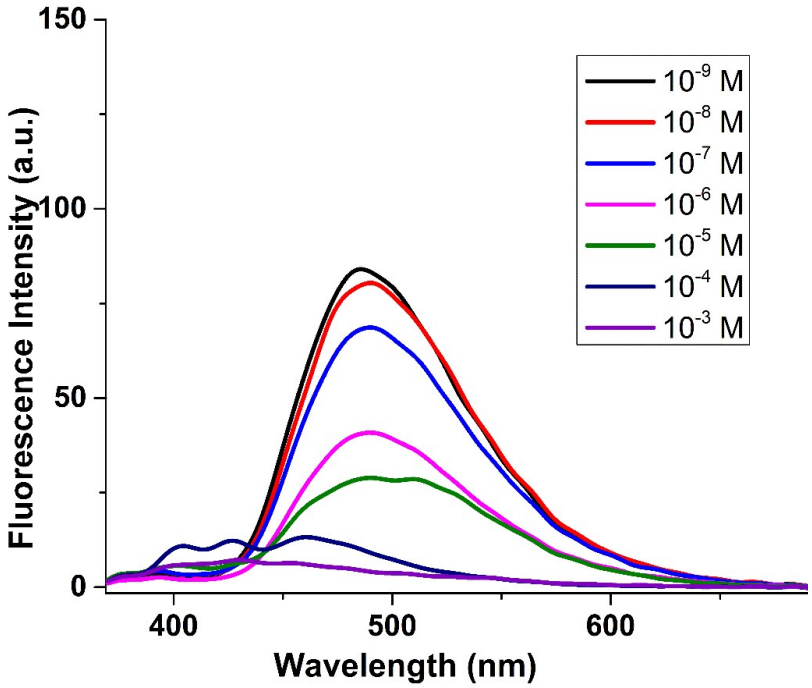

Fig. S3: Concentration dependent emission spectra of Probe P (10^{-3}–10^{-9} M solution in acetonitrile.

Limit of Detection (LOD)

The detection limit was calculated using Eq. 1.

$$LOD = \frac{3\sigma}{k} \qquad (1)$$

Where σ is the standard deviation of 10 consecutive scan of blank solution (Probe P, 20 µM) and k is the slope of a plot of emission intensity with metal ion concentration.

$$LOD = \frac{3 \times 1.54}{6.8014}$$

$$LOD = 0.679\ \mu M$$

So the limit of detection of probe P for zinc metal ion is 0.67 µM.

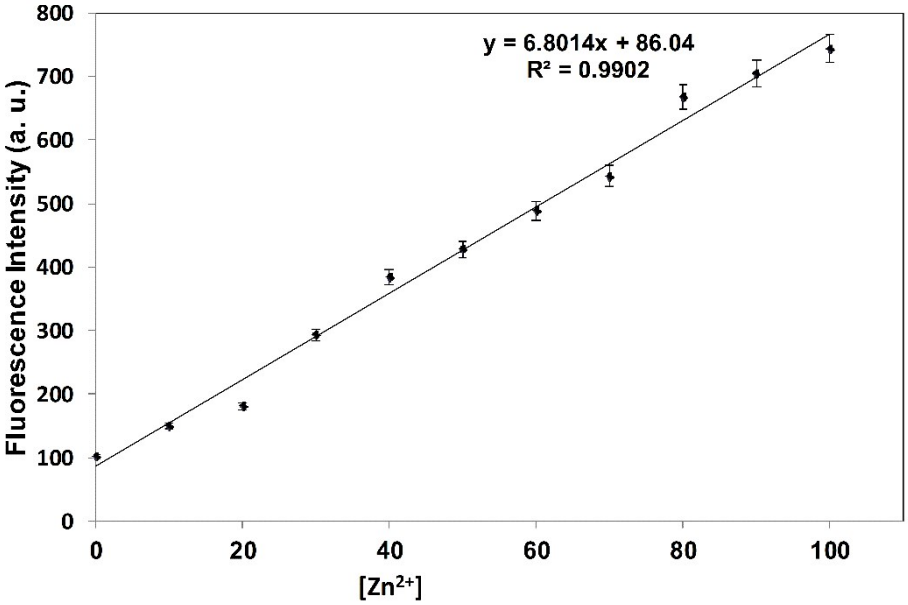

Fig. S4: Calibration curve for the calculation of detection limit for Zn^{2+} ion.

Job's Plot

Binding stoichiometry of Zn^{2+} complexes determined by Job's plot. In this method, equimolar solutions of P and Zn^{2+}(50 μM) were prepared in acetonitrile solvent and the absorbance were recorded with different mole fraction of chemosensor P and metal ion.

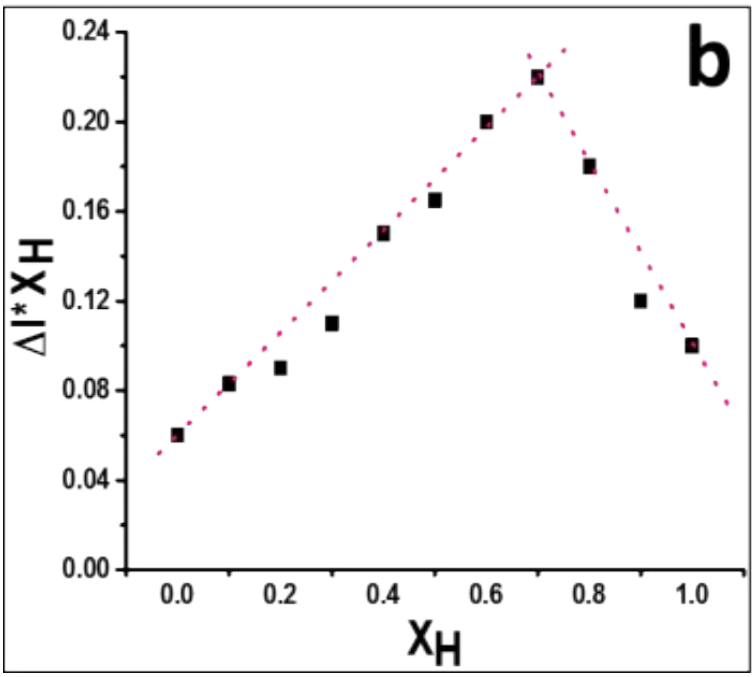

Fig. S5: Job's Plot.

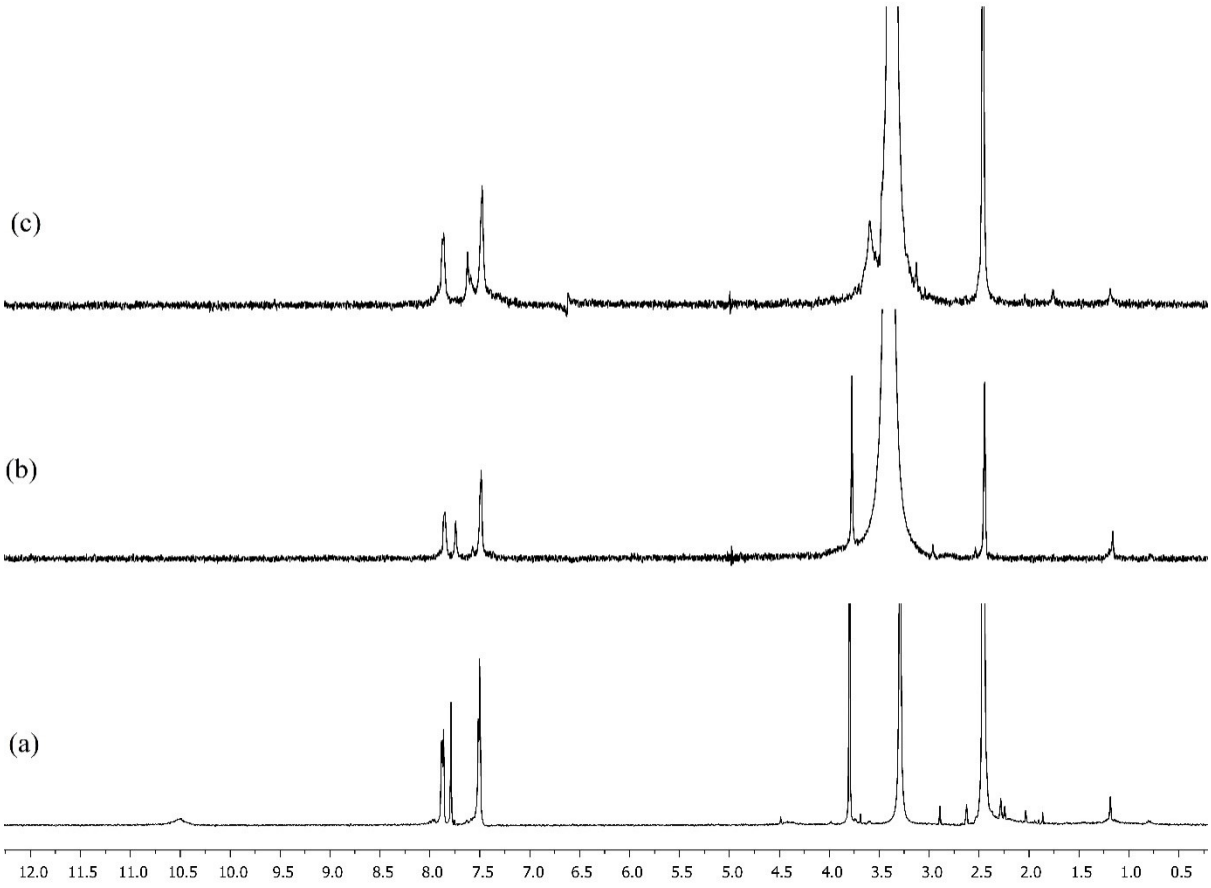

Fig. S6:^{1}H NMR spectra of P with and without Zn^{2+} DMSO-*d6*, 400 MHz; (a) probe P, (b) with 0.5 equi. of Zn^{2+}, (c) with 1 equi. of Zn^{2+} ion.

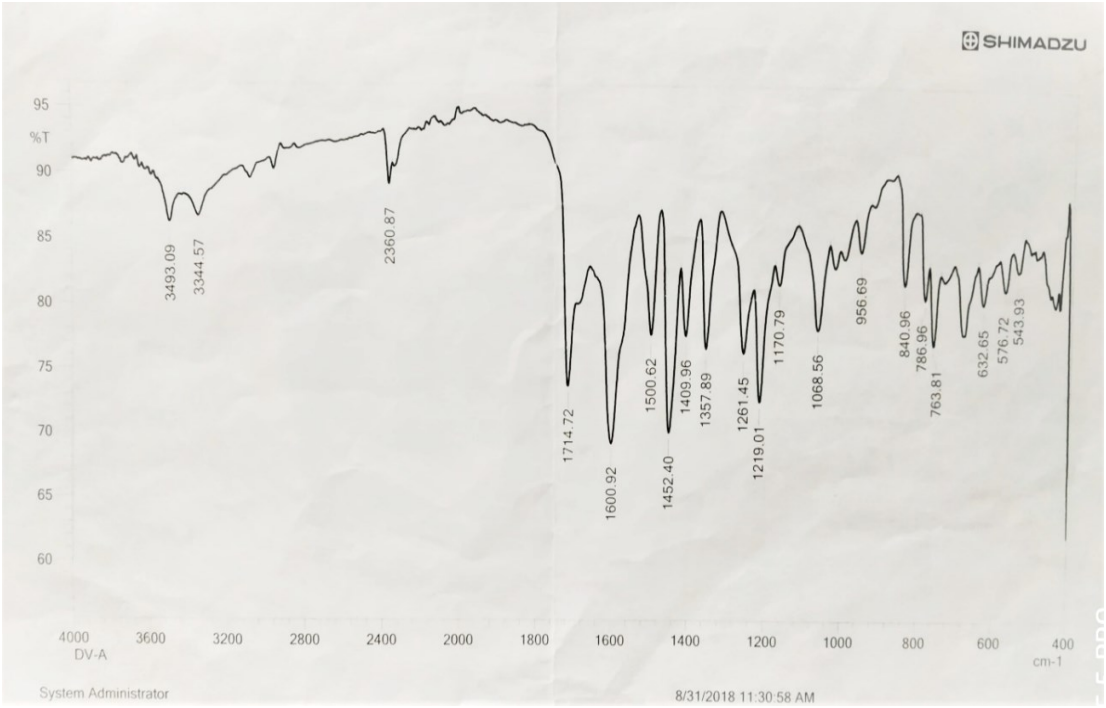

Fig. S7: FTIR spectrum of P.

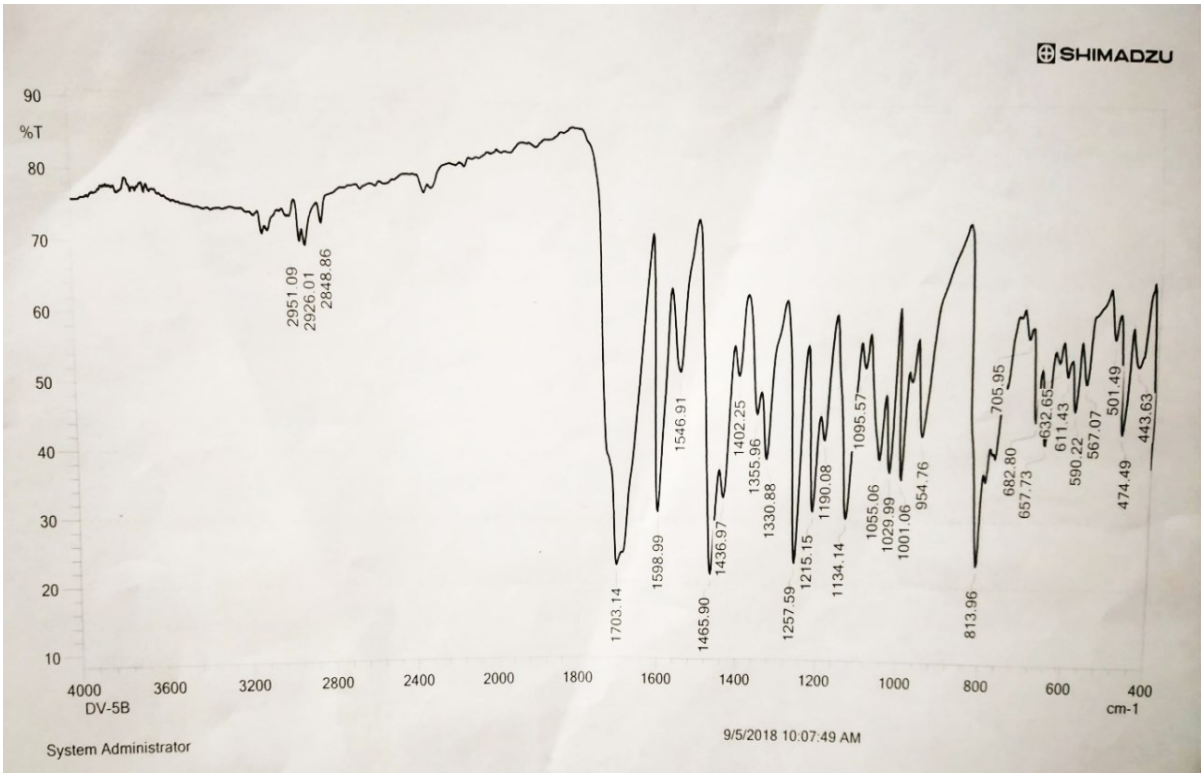

Fig. S8: FTIR spectrum of P-Zn^{2+} complex.

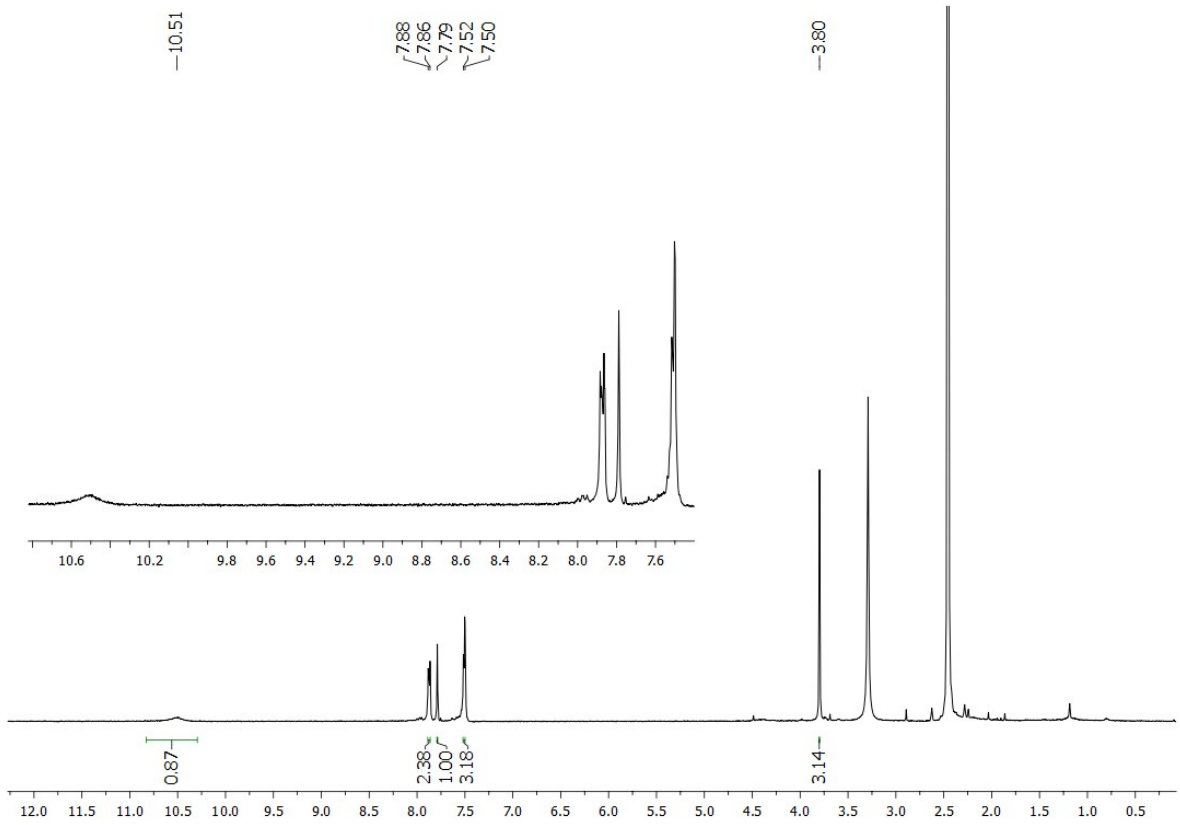

Fig. S9:^{1}H NMR spectrum of probe P.

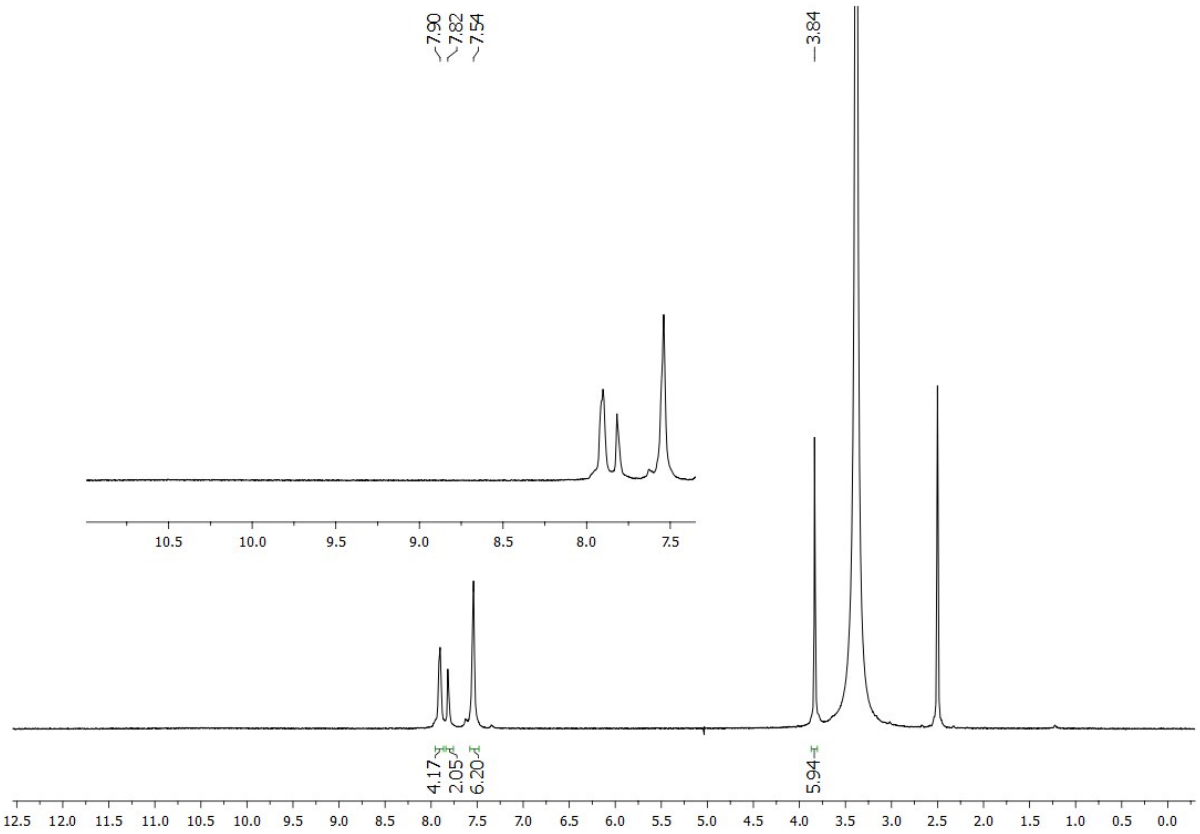

Fig. S10:^{1}H NMR spectrum of P-Zn^{2+} complex.

Table S2:Data of optimized geometries of probe P and P-Zn^{2+} complex.

compound	HOMO	LUMO	Band Gap (eV)
P	-7.938	-5.902	2.036
P-Zn^{2+}	-8.498	-8.336	0.161

Theoretical values at B3LYP/6-31G(d,p) and LANL2DZ level.

Quantum Yield

The relative fluorescence quantum yields were determined with quinine sulphate B (Φ_S = 0.54) in 0.1 M H_2SO_4 as a standard and calculated using the following equation 2.

$$\Phi_X = \Phi_S \times (I_X/I_S) \times (A_S/A_X) \times (\eta_X/\eta_S)^2 \qquad (2)$$

Where Φ represents quantum yield; A is absorbance at the excitation wavelength; λ_{ex} is the excitation wavelength; η is refractive index of the solution and subscripts x and s refer to unknown and standard samples respectively.

Table S3 Comparison of our work with previously reported literature.

Previously reported literature	Solvent	Detection limit	Aggregation phenomenon
Schiff base derivative of pyridoxal[2]	DMSO	0.87 μM	–
Pyrene pyridoxal[3]	DMSO	2.3 μM	–
Quinoline derivative[4]	DMF/H_2O (7/3, v/v)	10 μM	–
Schiff base derivative of Purine based[5]	Methanol	2 μM	–
Schiff base derivative of Julolidine[6]	DMF	3.3 μM	–
Schiff base derivative of Juloidine-imidazole[7]	DMF	15.6 μM	–
Tetrazolylpyridine[8]	H_2O	0.75 μM	–
Schiff base derivative of Crown ether .[9]	H_2O	1μM	–
Cyclam-Based "Clickates"[10]	Acetonitrile	75 μM	–
Porphyrin[11]	Ethanol	1.8 μM	–
Hydrazine[12]	DMF/H_2O	0.11 μM	AIEE
Terpyridine-based ligand[13]	DMSO/H_2O	–	AIE
This work	**Acetonitrile**	**0.67 μM**	**AIE**

References

1 M. Z. K.Baig, B.Prusti, D. Roy and M. Chakravarty**,** *ACS Omega* 2019, **4**, 5052–5063.

2 T. Anand, A. S. K. Kumar and S. K. Sahoo, *Photochem. Photobiol. Sci.,* 2018, **17**, 414–422.

3 Y. Upadhyay, T. Anand, L. T. Babu, P. Paira, G. Crisponi, A. K. S. Kumar, R. Kumar and S. K. Sahoo,*Dalton Trans.***,** 2018, **47**, 742–749.

4 Z. Dong, X. Le, P. Zhou, C. Dong and J. Ma, *RSC Adv.*, 2014, **4**, 18270–18277.

5 Pratibha, S. Singh,S. Sivakumarand S.Verma, *Eur. J. Inorg. Chem.* 2017, 4202–4209.

6 G. J. Park, Y. J. Na, H. Y. Jo, S. A. Lee, A. R. Kim, I. Noh and C. Kim, *New J. Chem.* 2014, **38**, 2587–2594.

7 Y. W. Choi, G. J. Park, Y. J. Na, H. Y. Jo, S. A. Lee, G. R. You and C. Kim, *Sensor Actuat B-Chem*2014, **194**, 343–352.

8 P.Kaleeswaran, I. A. Azath, V.Tharmaraj, and K. Pitchumani, *ChemPlusChem*2014, **79**,1361–1366.

9 D.A. Safin, M. G. Babashkina and Y. Garcia, *Dalton Trans.* 2013, **42**, 1969–1972.

10 Y. Lv, M. Cao, J. Li and J. Wang, *Sensors* 2013, **13**, 3131–3141.

11 E.Tamanini, K. Flavin, M. Motevalli, S.Piperno, L. A. Gheber, M. H. Todd, and M. Watkinson, *Inorg. Chem.* 2010, **49**, 3789–3800.

12 M.Shyamal, P.Mazumdar, S.Maity, S.Samanta, G. P. Sahoo, and A.Misra, *ACS Sens.* 2016, **1**, 739–747.

13 S. H. Jung, K. Y. Kwon and J. H. Jung, *Chem. Commun.*, 2015,**51**, 952–955.